

## CYCLIC BOND BEHAVIOUR OF FRP-TO-STEEL BONDED JOINTS

Hao Zhou, Yashar Doroudi, Dilum Fernando \*

School of Civil Engineering, The University of Queensland, Australia

\*Email: dilum.fernando@uq.edu.au

### ABSTRACT

Cyclic behaviour of the FRP-to-steel bonded interfaces is a key issue to be addressed in modelling the long-term performance of FRP-to-steel bonded joints. However, compared to extensive experimental and theoretical study on the bond-slip behaviour between two adherents, either FRP-to-steel or FRP-to-concrete under monotonic loading, so far only few research have been carried out on the cyclic behaviour of such bonded joints. This paper presents a new bond-slip model to model the behaviour of FRP-to-steel bonded joints under quasi-static cyclic loading. In addition, an analytical model to model the load-displacement behaviour and interfacial shear stress distributions is also presented. The results from the proposed model and the results from another existing model are compared with the experimental results from two FRP-to-steel bonded joints tests under cyclic loading. Results from the proposed model show a better agreement with the experimental load-displacement behaviour, shear stress distribution and the bond-slip behaviour.

### KEYWORDS

FRP-to-steel bonded joints, cyclic behaviour, interfacial shear stress distribution, bond-slip model.

### INTRODUCTION

In flexurally strengthened steel structures using externally bonded FRP laminates, the interfacial shear stress transfer in the adhesive layer that bonds the steel and FRP together is crucial to the performance of the strengthened structure (Teng *et al.* 2012). Therefore proper understanding of the bonded interfaces is of critical importance in determining when the failure will occur and how effectively the FRP is utilized. Many studies have been carried out on understanding and modelling the interfacial failures in FRP-to-steel bond joints (Yu *et al.* 2012, Fernando *et al.* 2015, Teng *et al.* 2015). Pull tests on simply bonded joints, where the adhesive layer is primarily subjected to interfacial shear stress, have been commonly used to study the bond behaviour under interfacial shear loading. Interfacial shear behaviour is an important basis for understanding the behaviour of FRP-to-steel interfaces subjected to combined shear and peeling stresses. A bond-slip model, which depicts the relationship between the local interfacial shear stress and the relative slip between the two adherents, is of fundamental importance to understand and model the behaviour of FRP strengthened steel structures. Many studies have been carried out to determine the bond-slip behaviour of FRP-to-steel bonded joints (Yu *et al.* 2012, Fernando *et al.* 2010); and different bond-slip models with different levels of sophistications have been proposed. Most commonly used are the bi-linear bond-slip models. In such models, when defining damage, linear unloading to zero stress at zero slip is assumed. Thus, any inelastic deformations are ignored. This assumption means, the applicability of such a bond-slip model is limited to static monotonic loading conditions. While no studies have been carried out on the bond-slip behaviour of FRP-to-steel bond joints under cyclic loading, some works have been done on FRP-to-concrete bonded joints under cyclic loading. In FRP-to-concrete bonded joints, debonding failure often occurs closer to the bonded interfaces few millimetres within the concrete, while debonding failures in FRP-to-steel bonded joints are unlikely to occur within the steel substrate due to the relatively high strength of steel. Due to this difference in debonding failure, direct application of the bond-slip models of FRP-to-concrete bonded joints to FRP-to-steel bonded joints is not possible. Nevertheless, underlying concepts such as interfacial fracture energy and effective bond length are still applicable to the FRP-to-steel bonded joints.

In the existing bond-slip models for FRP-to-concrete and FRP-to-steel bonded interfaces under quasi-static monotonic loading, damage parameter is calculated assuming linear unloading to zero load at zero stress. However, experimental results on the bond-slip behaviour of FRP-to-concrete bonded joints under cyclic loading showed remarkable hysteresis loops, indicating inelastic deformations occurred during the cyclic loading. In addition, experiments showed that the residual slip (i.e. slip at zero loading) at the loading end increased with the increase in loading cycles (Ko and Sato 2007). These observations clearly indicate that the commonly used approach of calculating the damage parameter in bond-slip models for quasi-static monotonic loading, i.e. assuming linear unloading to zero load at zero slip, is not accurate for cyclic loading. Based on the experimental

observations, several analytical approaches were proposed to define the bond-slip behaviour of the FRP-to-concrete bonded joints under cyclic loading (Ko and Sato 2007, Diab *et al.* 2009, Martinelli and Caggiano 2014, Carrara and De Lorenzis 2015). Except Ko and Sato (2007), the other existing models assume bi-linear bond-slip behaviour with a linear ascending branch followed by a linear descending branch, as commonly assumed in FRP-to-concrete bond-slip models under quasi-static monotonic loading. The essential difference between the different bond-slip models proposed for cyclic loading is in the approach used to define the damage parameter under cyclic loading. In the most advanced of these models (Martinelli and Caggiano 2014, Carrara and De Lorenzis 2015), damaged parameters is either related to the ratio between inelastic and total fracture energy (Martinelli and Caggiano 2014) or negative slip increments (i.e. reversal of the residual slip at zero shear stress) (Carrara and De Lorenzis 2015). Martinelli and Caggiano (2014) model assumes negative shear stresses to be possible during the unloading process while Carrara and De Lorenzis (2015) model assumes negative shear stresses are not possible. Negative shear stresses could occur due to the reversal of plastic deformations, friction or interlocking that are assumed to be negligible by Carrara and De Lorenzis (2015) in deriving their model. However, so far this assumption is not experimentally verified.

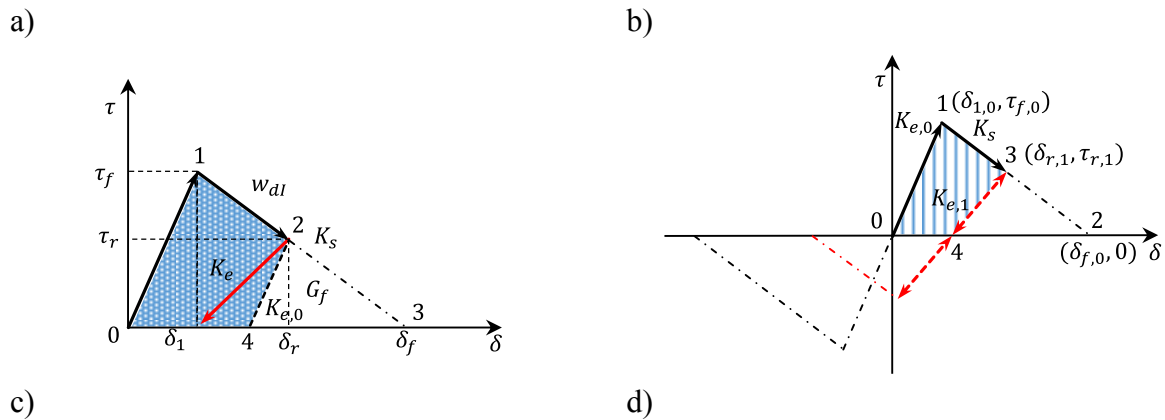
This paper presents an analytical model to model the behaviour of FRP-to-steel bonded joints under cyclic loading. The proposed model is similar to that proposed by Martinelli and Caggiano (2014), but different in terms of the damage parameter used. The analytical models are compared with preliminary experimental results from FRP-to-steel bonded joints carried out by the authors group.

## ANALYTICAL MODEL

In deriving the analytical solution presented below, few simplifying assumptions were made. It was assumed that the adhesive layer is subjected to only shear deformations. Previous experimental observations have found this assumption to be reasonable for a bond in a single shear pull off test (Fernando 2010). It is further assumed that the adhesive layer is subjected only to shear stresses which are constant across the adhesive layer thickness and that both adherents (i.e. the CFRP plate and the steel substrate plate) are subjected to uniformly distributed axial stresses. These assumptions have also been commonly adopted in the development of similar analytical solutions for CFRP-to-steel bonded joints under quasi-static monotonic loading (Fernando *et al.* 2014). With these assumptions, the governing differential equation well established for a bonded joints in a single-lap pull test is given by Fernando *et al.* (2014):

$$\frac{d^2\delta}{dx^2} - \left( \frac{1}{E_p t_p} + \frac{b_p}{E_s b_s t_s} \right) f(\delta) = 0 \quad (1)$$

Where  $\delta$  is the slip between the two adherents.  $E_p, t_p, b_p$  is the elastic modulus, thickness and width of the FRP plate respectively. Likewise,  $E_s, t_s, b_s$  is the elastic modulus, thickness and width of the steel plate respectively.  $f(\delta)$  represents the relationship between the shear stress ( $\tau$ ) and the slip ( $\delta$ ). Eq. 1 can be solved if the bond-slip model,  $f(\delta)$  is known. The bi-linear model under cyclic loading adopted in this study is illustrated in Figure 1.



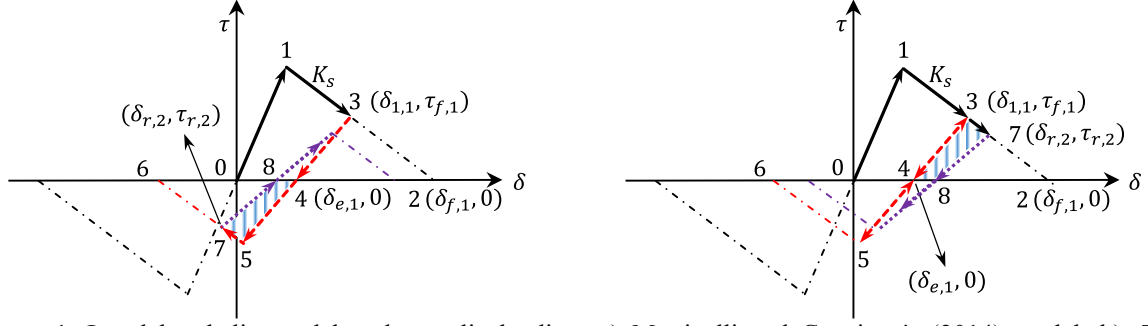


Figure 1. Local bond-slip model under cyclic loading: a) Martinelli and Caggiano's (2014) model; b): The proposed model in the first unloading (in softening range); c): The proposed model which subsequent unloading/reloading is in the negative softening range; d): The proposed model which subsequent unloading/reloading is in the positive softening range.

The local bond-slip model presented in Figure1 can be mathematically described as:

$$f(\delta) = \begin{cases} K_{e,i}(\delta - \delta_{e,i}) & \text{when } |\delta - \delta_{e,i}| \leq |\delta_{1,i} - \delta_{e,i}| \\ K_{e,i}(\delta_{1,i} - \delta_{e,i}) + K_s(\delta - \delta_{1,i}) & \text{when } |\delta_{1,i} - \delta_{e,i}| < |\delta - \delta_{e,i}| \leq |\delta_{f,i} - \delta_{e,i}| \\ 0 & \text{when } |\delta - \delta_{e,i}| > |\delta_{f,i} - \delta_{e,i}| \end{cases} \quad i = 0, 1, \dots, n \quad (2)$$

Where notation  $i$  means the  $i^{\text{th}}$  unloading/reloading step.  $\delta$  is the slip,  $\delta_{e,i}$  is the plastic slip, and  $\delta_{1,i}, \delta_{f,i}$  is the slip value corresponding to the peak shear stress and debonding initiation respectively.  $K_{e,i}$  is the damaged elastic stiffness which is given by:

$$K_{e,i+1} = (1 - D_{i+1})K_{e,i} \quad i = 0, 1, \dots, n \quad (3)$$

When  $i=0$ ,  $K_{e,0}$  represents the initial elastic stiffness. It is also assumed that when unloading/reloading occurs in the elastic range, no damage would be caused. Otherwise, the damage parameter  $D$  is used to indicate the stiffness degradation.

The plastic slip is calculated as:

$$\delta_{e,i} = \delta_{1,i} - \frac{\tau_{f,i}}{K_{e,i}} \quad i = 0, 1, \dots, n \quad (4)$$

In which  $\tau_{f,i}$  is the peak shear stress value in the  $i^{\text{th}}$  unloading/reloading step, which is also the shear stress value when unloading happens in the previous step, assuming unloading happens in the softening range. Otherwise, it might keep unchanged.

In terms of the damage parameter, Martinelli and Caggiano (2014) defined the damage parameter as a function of the ratio between the inelastic energy and the total fracture energy, i.e.

$$D_I = \left( \frac{w_{dl}}{G_f} \right)^{\alpha_d} \quad (5)$$

Where  $\alpha_d$  is a damage coefficient, which is taken to be a unit in the subsequent analysis. In Figure 1a,  $w_{dl}$  is indicated by the area enclosed by the bond-slip curve and the line with slope of the initial stiffness, i.e.  $A_{01240}$ . However, with this definition of the damage parameter, when damage parameter value is closer to zero, negative slip may result at zero shear stress during the unloading. The negative residual slip means total fracture energy may increase, which is not possible. In the current study an alternative damage parameter is defined as follows,

$$D_{II,i+1} = \left( \frac{w_{dII,i+1}}{G_i} \right)^{\alpha_d} \quad (6)$$

As graphically shown in Figures 1b-d, the calculation of the damage parameter can be explained as follows. Since no damage is considered when unloading happens in the elastic range, only the situation that unloading/reloading in the softening range is illustrated.

In Figure 1b, assuming the first unloading occurs, therefore

$$w_{dII,1} = A_{01340} = A_{013240} - A_{4324} \quad (7)$$

$$G_0 = A_{013240}$$

In Figure 1c, if the reloading happens in the negative softening range,

$$w_{dII,2} = A_{45784} = A_{4576084} - A_{87608} \quad (8)$$

$$G_1 = A_{4576084}$$

Or as shown in Figure 1d, reloading/unloading in the positive softening range,

$$w_{dII,2} = A_{43784} = A_{437284} - A_{8728} \quad (9)$$

$$G_1 = A_{437284}$$

Note  $A_{4324} = A_{4576084}$  in Figure 1c and  $A_{4324} = A_{437284}$  in Figure 1d, when it comes to failure, the total energy dissipated in the cracks and plastic deformation is equal to the total fracture energy which is the area under the initial bond-slip relationship (Bažant 1996), i.e.

$$\sum_{i=1}^n w_{dII,i} = G_f = A_{013240} \quad (10)$$

In a particular unloading/reloading case,  $w_{dII,i}$  can be expressed implicitly as:

$$w_{dII,i+1} = G_i - \frac{1}{2} \left[ \delta_{f,i} - \delta_{r,i+1} + \tau_{r,i+1} / K_{e,i+1} \right] \tau_{r,i+1} \quad (11)$$

Substituting Eq. 4 into Eq. 6, it is straightforward to get an implicit expression of the damage parameter, i.e.

$$1 - D_{II,i+1} = \frac{1}{2G_i} \left\{ \delta_{f,i} - \delta_{r,i+1} + \tau_{r,i+1} / \left[ (1 - D_{II,i+1}) K_{e,i} \right] \right\} \tau_{r,i+1} \quad (12)$$

It can be found that the damage parameter is the only variable, which can be calculated given a slip value. Obviously, the damage parameter and the unloading/reloading stiffness is a function of the slip value while unloading/reloading occurs in both models. Meanwhile, it is assumed that when the slip is reversed, the bond-slip model is antisymmetric respect to the point where the shear stress is zero at the elastic range, i.e. point 0 in the initial bond-slip model and point 4 in the unloading one. Besides, the stiffness in the softening range keeps constant. The difference between these two prediction models will be explained and discussed in the case study.

## EXPERIMENT

Series of single-shear pull off test on CFRP-to-steel bonded joints were carried out at the University of Queensland (UQ) structures laboratory. Two of these tests are used in this study for the comparison with analytical results. Both specimens were made using 1.4mm thick, 50mm wide CFRP plates bonded to steel substrate with 1mm thick Sika 30 adhesive layer. The elastic modulus of CFRP in the fiber direction was 170GPa. Details of the specimens and the test setup are given in Figure 2.

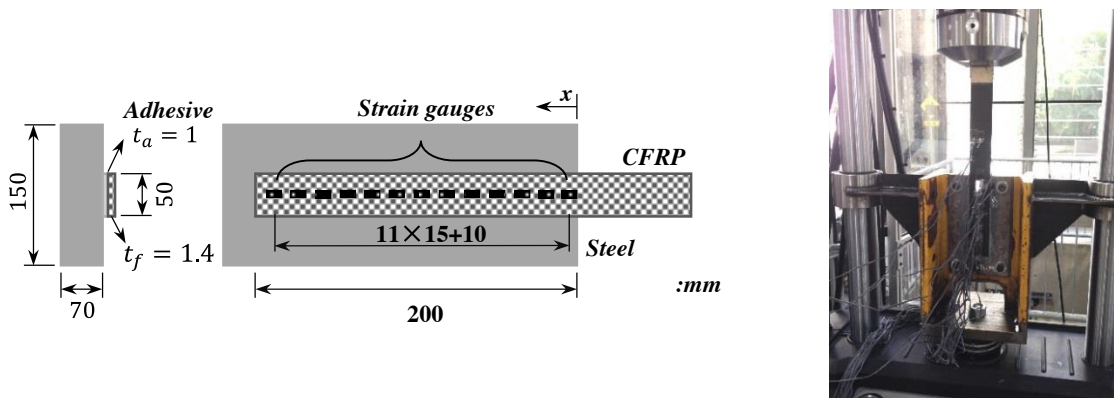


Figure 2 Test set-up and instrumentation

Both specimens were nominally identical and varied only in the applied loading scheme. For the first specimen (Specimen I), fully reversed load cycles were applied, while for the second specimen (Specimen II) partially reversed load cycles were applied. The loading schemes for specimen I and II are given in Table 1. These loading schemes were designed based on the analytical full range behaviour models (Fernando *et al.* 2014) to obtain; (1) several loading cycles within the ascending branch of local bond-slip models, (2) several load cycles within the descending branch of local bond-slip models, (3) several cycles with shear stress zero (or below zero) during unloading (for fully reversed load cycles only), and (4) several cycles with positive shear stress at

reloading (for partially reversed loading cycles only). A number of strain gauges were attached to the top surface of the CFRP plate at intervals of 15mm except for the first strain gauge (counted from the loaded end of the steel substrate, see Figure 2, which was at 5mm from the loaded end of the steel substrate plate and the second one was 10mm interval.

Based on a series of monotonic test, the parameters associated with the bond-slip model were identified as  $\delta_i = 0.04mm$ ,  $\delta_f = 0.13mm$ ,  $\tau_f = 23MPa$ . Using these values in the bond-slip model presented in Eq. 2, the governing equation, i.e. Eq. 1 was solved numerically to get the load-displacement curve under cyclic loading, the shear stress distribution along the bonding length and the local bond-slip relationship under cyclic loading.

Table 1 The loading scheme

Loading step	Fully reversed	Partially reversed
	mm→mm→mm	kN→mm→kN
1	0→0.042→0(0.002)	0→0.043→2.6
2	0(0.002)→0.062→0(0.005)	2.6→0.077→18
3	0(0.005)→0.082→0(0.008)	18→0.221→28
4	0(0.008)→0.112→0(0.012)	28→0.255→28
5	0(0.012)→0.162→0(0.009)	28→0.292→28
6	0(0.009)→0.234→0(0.012)	28→0.332→28
7	0(0.012)→0.320→0(0.014)	28→0.370→28
8	0(0.014)→0.416→0(0.009)	28→0.404→28
9	0(0.009)→0.6	28→0.438→28
10	N/A	28→0.477→28
11	N/A	28→0.542→28
12	N/A	28→0.587→38

Note: The slip value in the bracket is the minimum slip reached in the test while unloading.

## RESULTS AND DISCUSSION

The experimental load vs displacement curves for both specimens are compared with the analytical predictions in Figure 3. Results from the Martinelli and Caggiano (2014) model are shown as Prediction-I, while the results from the proposed model in this study are shown as Prediction-II. Both Prediction-I and Prediction-II generally agree well with the experimental curves. Hysteresis loops while unloading and reloading can be observed from the test results. Such hysteresis loops are ignored in the simplified analytical models presented in this study.

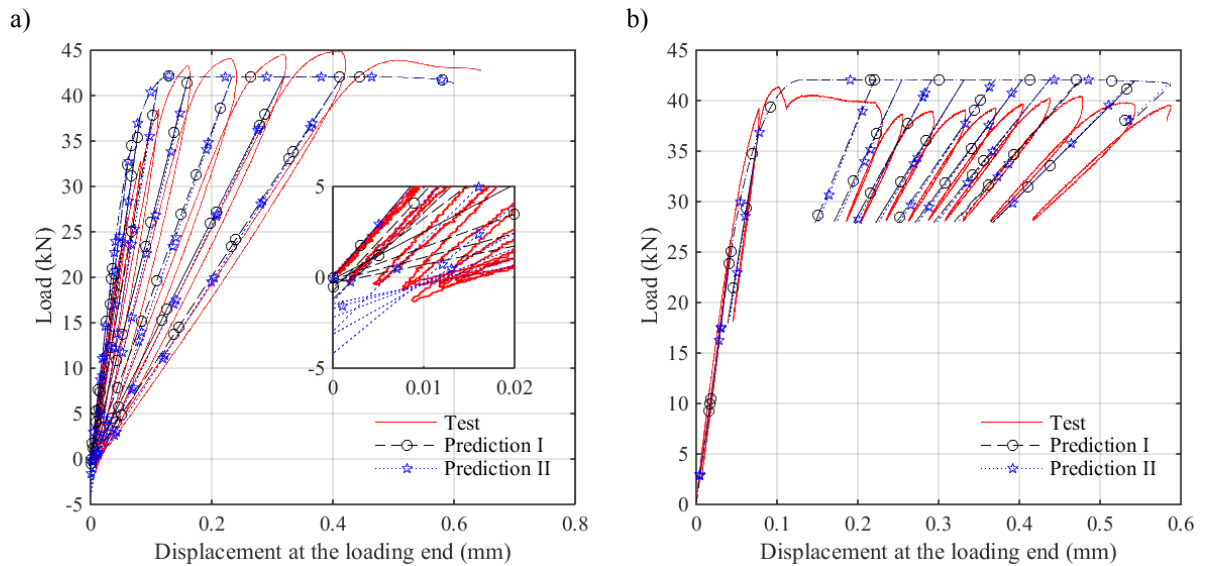
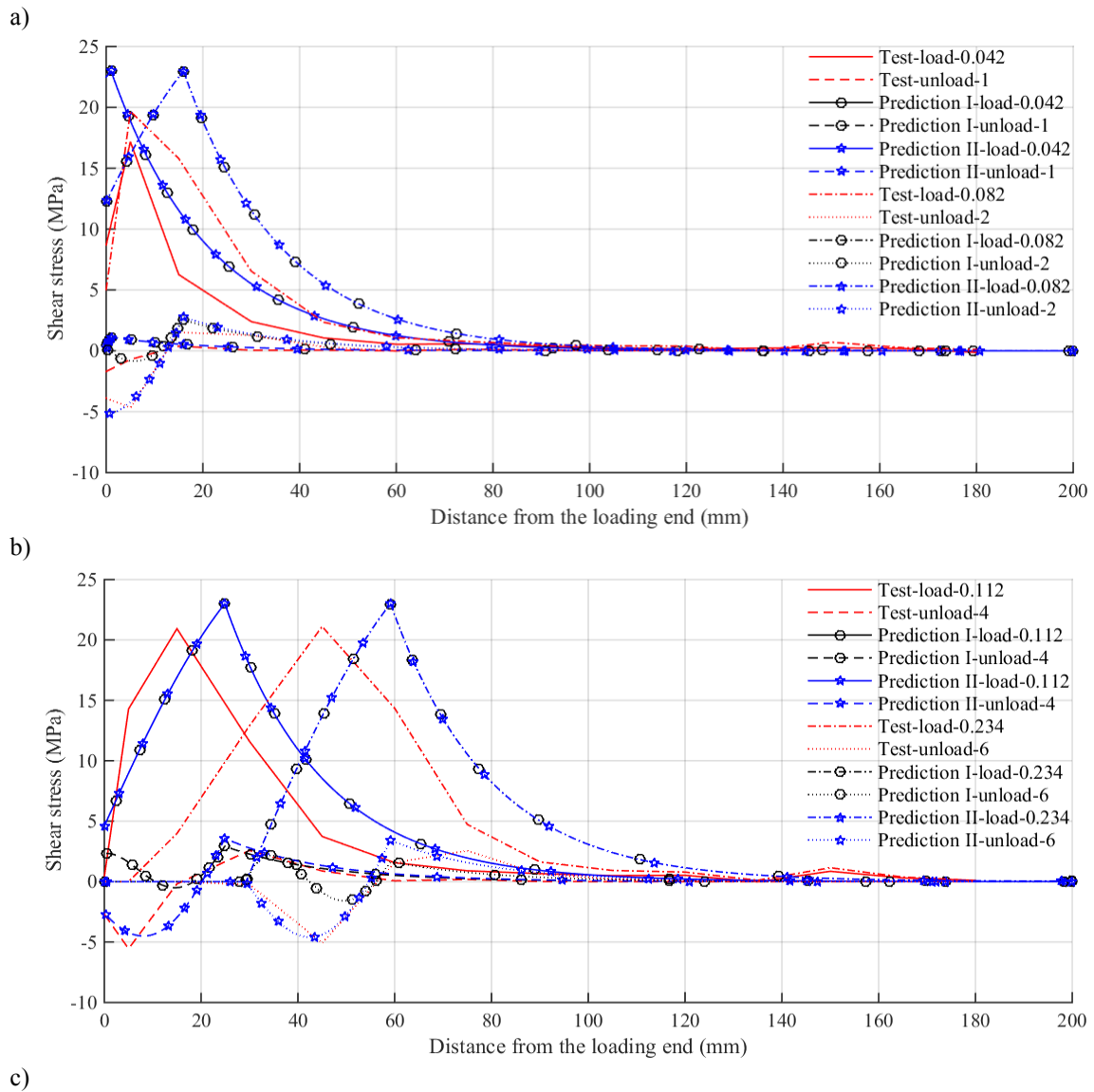
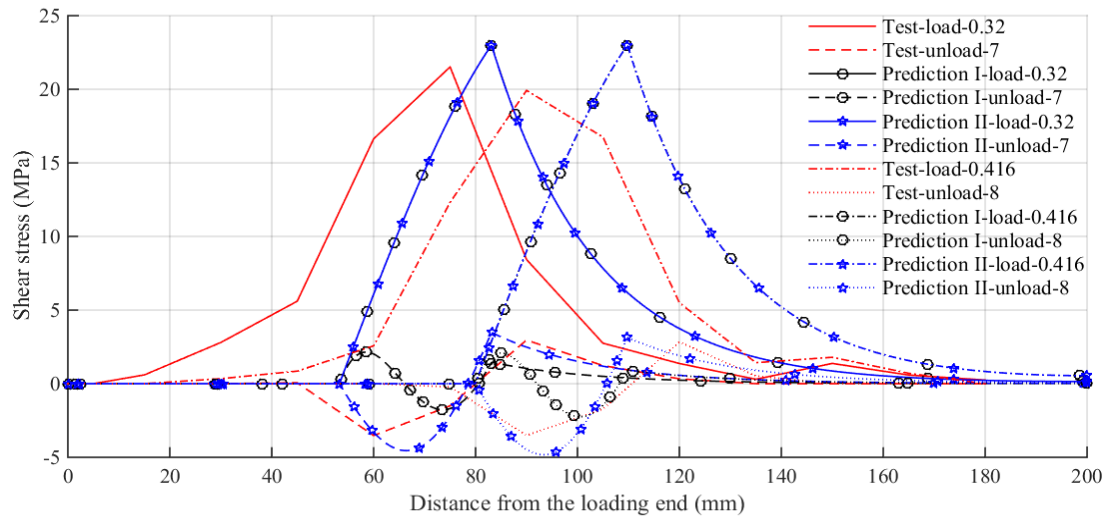


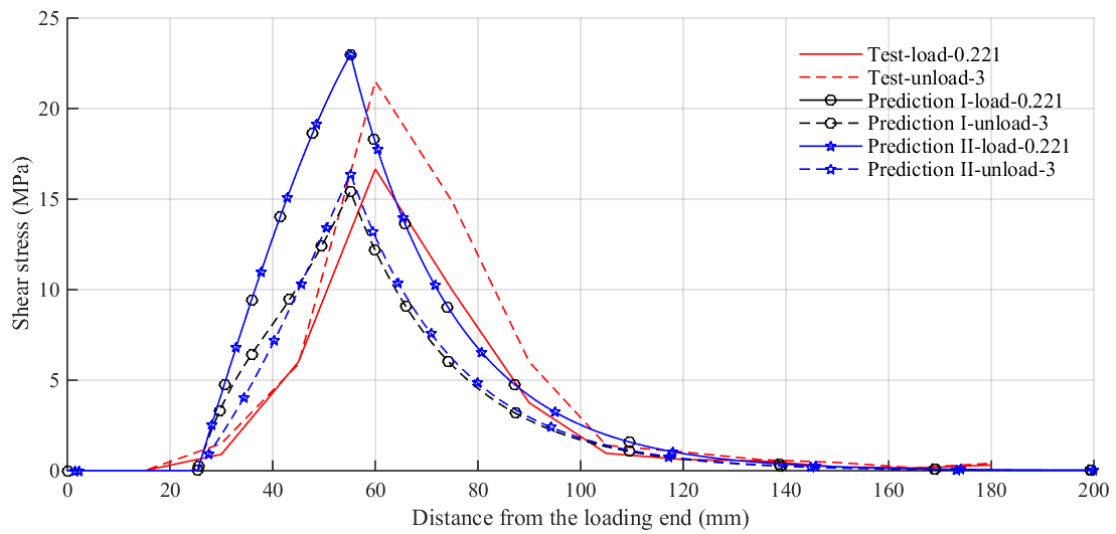
Figure 3 The comparison between the theoretical and experimental results: (a) fully reversed cyclic loading ; (b) partially reversed cyclic loading

A detailed illustration of the load-displacement curve close to the origin is presented in Figure 3a. Results show that the external force is negative when the displacement at the loaded end approaches zero. Due to the reduced stiffness of the unloading path in damaged regions, a residual slip can be expected at zero load. Further reduction in the displacement at the loaded end will result in negative loading. In this negative load region, Prediction-II gives a better agreement with the experimental results than the Prediction-I (Figure 3a). Occurrence of the negative loading can be further explained by the shear stress distribution along the bond length as shown in Figure 4.





d)



e)

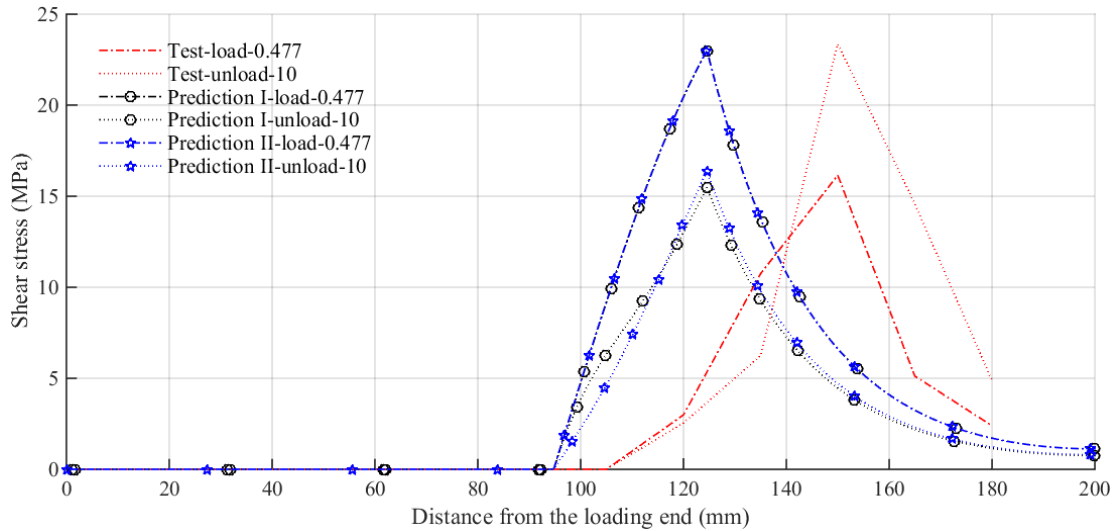


Figure 4 The shear stress distribution comparison between test and both predictions: a) to c) comparison based on the fully reversed cyclic loading test results; d) to e) comparison based on the partially reversed cyclic loading test results

The experimental interfacial shear stress distributions of fully reversed cycle loading test show negative shear stresses at the loaded end and positive shear stresses in the region following the negative shear region (Figures 4a-c) at full unloading (according to the slip in the test). Negative shear stresses mean that the direction of the



shear has reversed, which is due to the reversal of the plastic slip in the region closer to the loaded end. It is also seen that closer to the zero loading, the area of negative shear stress region is larger than the positive shear stress region, thus agreeing with the negative loading observed in the load displacement curve at the reversal of residual displacement. The difference between the negative stress region and positive stress region becomes more pronounced as the load increases. Prediction-II captures this negative stress region effectively while prediction-I always predicts positive stresses closer to the loaded end (Figures 4a-c) except in the initial loading cycles. During the positive loading, both models give similar predictions and agree well with the experimental results at lower loads. As the load increases, predicted interfacial shear stress distributions are found to be shifted towards the unloaded end compared to the experimental interfacial shear stress distributions. For the partially reversed cyclic loading test, both prediction-I and prediction-II give similar predictions (Figure 4d). As negative shear stresses does not exist, both models appear to agree well with the experimental results. Load displacement curve of the specimen I shows that experimental load to be slightly higher than the predicted load, and initial stiffness of the load displacement curve to be slightly lower than the initial stiffness of the predicted curve. These differences could be explained through the comparison of local bond-slip models.

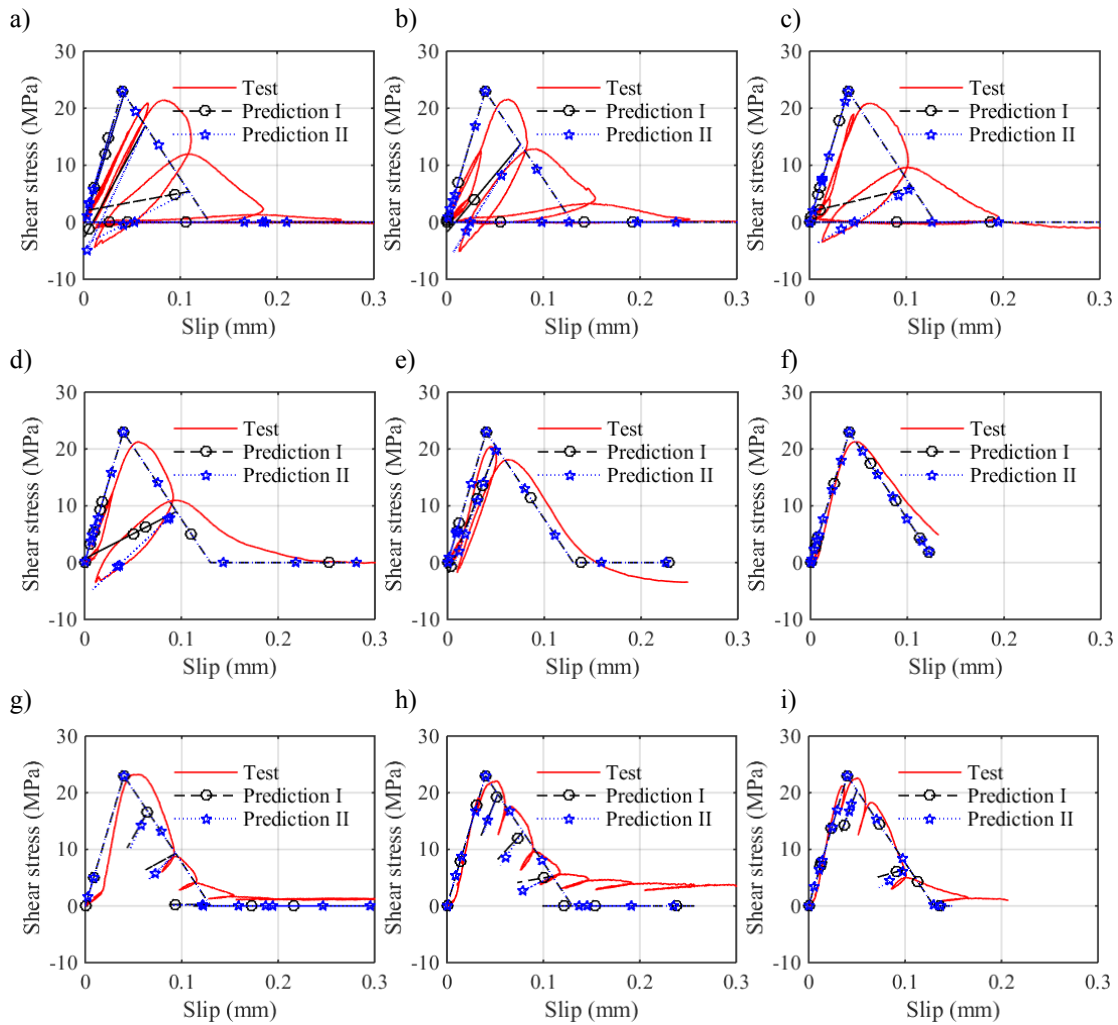


Figure 5 The evolution of local bond-slip model at different points along the bonding length: i.e. fully reversed cyclic loading: a)  $l=15\text{mm}$ ; b)  $l=45\text{mm}$ ; c)  $l=60\text{mm}$ ; d)  $l=90\text{mm}$ ; e)  $l=105\text{mm}$ ; f)  $l=135\text{mm}$ ; partially reversed cyclic loading: g)  $l=45\text{mm}$ ; h)  $l=90\text{mm}$ ; i)  $l=120\text{mm}$

A comparison between the predicted and experimental bond-slip curves at different locations along the bond length for specimen I is given in Figures 5a-f, while those for specimen II are given in Figures 5g-i. Significant hysteresis loops can be seen in the experimental bond-slip curves of specimen I, compared to the specimen II. Such hysteresis behaviour is neglected in the prediction models. Both prediction models over-estimate the initial stiffness of the bond-slip curves. This over estimation results in the overestimation of load-displacement behaviour. In addition, it can also be seen that the maximum slip, where the debonding initiation occurs, is significantly under estimated by the bond-slip models. This under-estimation of the maximum slip result in early debonding in the prediction models compared to the experimental result, which is demonstrated by the shift in



interfacial shear stress distributions in Figure 4. Compared to prediction-I results, prediction-II results give a much better agreement with the experimental bond-slip behaviour under cyclic loading, especially after the damage initiation. After the damage initiation, during unloading, prediction-I is shown to give negative slip at zero stress, which is thermodynamically not possible. Prediction-II does not show such errors, and always results in a positive residual slip at zero shear stress.

## CONCLUSIONS

This paper has presented an analytical bond-slip model for FRP-to-steel bonded joints under quasi-static cyclic loading. An analytical model to model the behaviour of FRP-to-steel bonded joints under quasi-static cyclic loading is also presented. Results from the proposed model and Martinelli and Caggiano (2014) model are compared with the experimental results from two FRP-to-steel bond joints tests under cyclic loading. Based on these comparisons, some conclusions can be drawn as follow: 1) both prediction models show a good agreement of the load-displacement relation of FRP-to-steel joints under both full and partial cyclic loading, but proposed model is superior to the existing model in terms of predicting the behaviour when slip at the loaded end is closer to zero during the unloading. 2) the results from the proposed model show a good agreement of the shear stress distribution, compared to an opposite distribution trend in Martinelli and Caggiano (2014) model. 3) more research is required to construct the constitutive model of such kind of bonding joints under cyclic loading, with regard to the bond behaviour at the interface level.

## ACKNOWLEDGMENTS

Authors would like to thank technicians at the UQ structures lab for their help in carrying out experimental tests.

## REFERENCES

- Bazant, Z. (1996). "Analysis of work-of-fracture method for measuring fracture energy of concrete". *Journal of Engineering Mechanics*, 122(2), 138-144.
- Carrara, P. and De Lorenzis, L. (2015). "A coupled damage-plasticity model for the cyclic behavior of shear-loaded interfaces". *Journal of the Mechanics and Physics of Solids*, 85(1), 33-53.
- Diab, H. M., Wu, Z. and Iwashita, K. (2009). "Theoretical solution for fatigue debonding growth and fatigue life prediction of FRP-concrete interfaces". *Advances in structural engineering*, 12(6), 781-792.
- Fernando, D. 2010. Bond behaviour and debonding failures in CFRP-strengthened steel members. PhD, The Hong Kong Polytechnic University, HongKong, China.
- Fernando, D., Yu, T. and Teng, J. G. (2015). "Behavior and modeling of CFRP-strengthened rectangular steel tubes subjected to a transverse end bearing load". *International Journal of Structural Stability and Dynamics*, 15(8), 1540031-1-24.
- Fernando, D., Yu, T. and Teng, J. G. (2014). "Behaviour of CFRP laminates bonded to a steel substrate using a ductile adhesive". *Journal of Composites for Construction*, 18(2), 04013040.
- Fernando, D., Yu, T., Teng, J. G. and Zhao, X. L. (2010). "Experimental behavior of CFRP-to-steel bonded interfaces". *11th International Symposium of Structural Engineering*, 18-20 December, Guangzhou, China.
- Ko, H. and Sato, Y. (2007). "Bond stress-slip relationship between FRP sheets and concrete under cyclic load". *Journal of Composites for Construction*, 11(4), 419-426.
- Martinelli, E. and Caggiano, A. (2014). "A unified theoretical model for the monotonic and cyclic response of FRP strips glued to concrete". *Polymers*, 6(2), 370-381.
- Teng, J. G., Fernando, D. and Yu, T. (2015). "Finite element modelling of debonding failures in steel beams flexurally strengthened with CFRP laminates". *Engineering Structures*, 86(1), 213-224.
- Teng, J. G., Yu, T. and Fernando, D. (2012). "Strengthening of steel structures with fiber-reinforced polymer composites". *Journal of Constructional Steel Research*, 78(1), 131-143.
- Yu, T., Fernando, D., Teng, J. G. and Zhao, X. L. (2012). "Experimental study on CFRP-to-steel bonded interfaces". *Composites Part B: Engineering*, 43(5), 2279-2289.